Bright Band Gap Photoluminescence from Unprocessed Single-Walled Carbon Nanotubes

J. Lefebvre,[1] Y. Homma,[2] and P. Finnie[1]

[1]*Institute for Microstructural Sciences, National Research Council, Building M-50, Montreal Road, Ottawa, Ontario, K1A OR6, Canada*

[2]*NTT Basic Research Laboratories, 3-1 Morinosato-Wakamiya, Atsugi, Kanagawa 243-0198, Japan*

(Received 7 March 2003; published 27 May 2003)

Unprocessed single-walled carbon nanotubes suspended in air at room temperature emit bright, sharply peaked band gap photoluminescence. This is in contrast with measurements taken from nanotubes lying on the flat surface for which no luminescence was detected. Each individual nanotube has a luminescence peak of similar linewidth (~ 13 meV), with different species emitting at various different wavelengths spanning at least 1.0 to 1.6 μm. A strong enhancement of photoluminescence intensity is observed when the excitation wavelength is resonant with the second Van Hove singularity, unambiguously confirming the origin of the photoluminescence.

DOI: 10.1103/PhysRevLett.90.217401 PACS numbers: 78.67.Ch, 78.55.–m, 78.66.Tr, 81.07.De

Single-walled carbon nanotubes (SWNTs), now known to exhibit many remarkable physical properties, are perhaps the most widely investigated nanostructures and are expected to have uses in electronics and other applications [1,2]. Their structure can be classified by (n, m) indices which uniquely specify diameter and chirality. Two-thirds of (n, m) classes are expected to be direct band gap semiconductors [3,4]. Being one-dimensional materials, the SWNT density of states (DOS) is characterized by Van Hove singularities and for the semiconducting tubes the DOS is therefore sharply peaked at the band gap [5–7]. Theoretically, then, nanotubes should show strong band gap photoluminescence (PL). However, only very recently has such band gap PL from SWNTs been observed, and then only in processed and purified nanotubes coated by soap micelles in solution [8,9]. Here we show that bright band gap PL can be obtained from unprocessed, bare SWNTs in air at room temperature. The reason that PL has been elusive until now will be further clarified. The methods described will enable PL and related optical techniques to be applied quite generally to the SWNT material system. In addition to its fundamental importance, the fact that sharply peaked, bright PL is obtained at room temperature from 1.0 to 1.6 μm, and most probably beyond, suggests that SWNTs could have applications in optoelectronics.

In SWNTs all the constituent atoms are surface atoms. As a consequence, the electronic properties of nanotubes are strongly influenced by their environment [10,11]. It is necessary therefore to isolate the nanotubes. To date, reports of SWNT band gap PL required chemical unbundling of initially aggregated nanotubes [8]. In that case, it was possible to observe PL only for SWNTs surrounded in soap micelles, which served to separate the nanotubes. Rather than beginning with such bundles and subsequently processing them, here we use chemical vapor deposition (CVD) on patterned substrates to obtain isolated SWNTs from the outset.

In order to prevent contact between the tube walls and other materials, arrays of pillars (nominally 100 nm in diameter, 360 nm high, 500 nm spacing) were used as supports for SWNTs [12]. The patterns were prepared on conventional (100) oriented silicon substrates using synchrotron-radiation lithography. For nanotube CVD catalysis a thin layer of iron or cobalt (~ 1 nm) was deposited on the patterns by e-beam evaporation at normal incidence, covering everything except the sides of the pillars. We explicitly present results only for iron; however, the PL was similar for both catalysts.

A pure methane CVD process was used to grow SWNTs [13,14]. At high temperatures thin iron films break up into small particles ideal for catalysis [12]. Samples were heated to between 800 and 900 °C, in a 300 sccm (cubic centimeters per minute at standard temperature and pressure) flow of argon at 66.5 kPa, after which methane was substituted for argon at the same pressure and flow rate. Samples were exposed to methane for 1 min, after which the heat was shut off, the gas flow stopped, and the gas pumped out. Samples were then removed to air. Control samples without nanotubes were made by the above process using argon only, rather than introducing methane.

A scanning electron microscope (SEM) image of the silicon pillars and grown SWNTs is shown in Fig. 1. The image is taken from an angle ($\sim 30°$). Suspended nanotubes are clearly seen extending from the silicon pillars, with most bridging pillar to pillar. Much more difficult to see, there are also abundant nanotubes lying on the bottom flat surface and on the unpatterned areas of the sample. There are strong selection effects associated with SEM imaging of nanotubes: suspended nanotubes may be clearly visible, while those lying on the surface may show almost no contrast. It is shown below that PL is also very selective.

For PL measurements, two optical configurations were used: micro-PL (μPL) and macro-PL (MPL). In the μPL

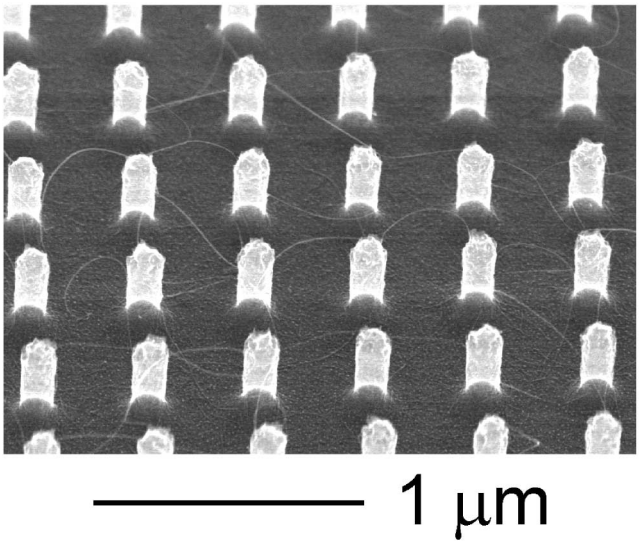

FIG. 1. Scanning electron micrograph of nanotubes on pillars. An array of silicon pillars is shown from an angle ($\sim 30°$). Single walled nanotubes are clearly seen bridging the pillars. On close inspection, some tubes lying on the surface below can also be seen.

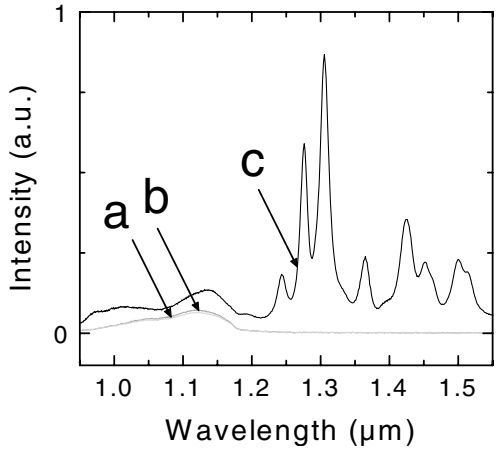

FIG. 2. Photoluminescence spectra: (*a*) from the pillar areas of an argon-only control sample; (b) on flat areas of a methane CVD sample with abundant nanotubes; (*c*) on pillar areas of methane CVD samples with bridging nanotubes. Spectra were taken at room temperature in air with the μPL configuration (see text), using a HeNe laser (633 nm) at 1.7 mW, with a 2 μm diameter spot.

configuration, excitation and collection were normal to the surface through a microscope objective, for a 2 μm diameter excitation spot size. In the MPL configuration, the luminescence was collected at normal incidence, and excitation was at off normal incidence, with a 100 μm excitation spot size. In both cases, the luminescence was detected by a liquid nitrogen cooled InGaAs photodiode array on a single grating spectrograph with up to 0.25 meV resolution. Spectra were accumulated over periods of about 1 min. A variety of lasers were used to excite at different wavelengths. The sample rested on a movable stage with micron accuracy, making it possible to repeatedly return to the same position.

All PL spectra shown were obtained at room temperature in air. Typical PL spectra are shown in Fig. 2. These were taken with a HeNe laser at 633 nm, with the μPL setup (2 μm spot diameter) and 1.7 mW excitation power. The line labeled "*a*" is the PL of a nanotube-free control sample. For this sample, the luminescence signal is just that which comes from the iron coated silicon pillar area. Line "*b*" is the PL from a methane CVD sample with abundant nanotubes taken in a flat area without any pillars. There is essentially no difference between this and the pillar areas of the control sample. Line "*c*" is the PL from the same CVD sample but with the laser spot moved to the pillar areas. Several narrow peaks are seen, and we identify them as arising from the band gap PL of suspended tubes.

The laser spot is large enough that it samples about a dozen pillars at a time. Translating the spot across the pillar areas, various infrared peaks of similar linewidths (~ 13 meV) appear and disappear. Returning to the same spot always results in the same spectrum, and across the sample several particular wavelengths appear again and again. Depending on precise diameter and chirality, SWNTs of order 1 nm in diameter, like those suspended here, are expected to have band gaps throughout the infrared band. We thus identify the many different PL peaks as band gap emission from suspended SWNTs of many different diameters and chiralities. Each individual peak corresponds to a specific suspended SWNT.

Next we confirm this identification with the use of resonant excitation, following Ref. [9]. This technique exploits the multiple Van Hove singularities in the density of states expected for one-dimensional confinement. Absorption of the exciting beam can be strongly enhanced by choosing an excitation wavelength resonant with the abundantly available states at the second order set of Van Hove singularities. As in the nonresonant case, the PL comes after carriers relax and recombine at the lowest energy Van Hove singularities at the band gap. For SWNTs the ratio of first to second singularity wavelength is on average ~ 1.7, depending somewhat on chirality [8,9]. It is therefore expected that, when averaging over an evenly distributed ensemble of many (n, m) species, PL emission should be resonantly enhanced in a band around 1.7 times the excitation wavelength.

To vary the excitation wavelength a variety of lasers were used. Continuous wave (CW) and pulsed wave (PW) lasers were used for the experiment: a frequency doubled YAG laser at 532 nm (CW); a HeNe laser at 633 nm (CW); semiconductor laser diodes at 670, 785, 830, and 860 nm (CW); a Ti:sapphire laser at 808 nm (CW and PW, 130 fs pulse duration, 82 MHz repetition rate); a tunable frequency doubled optical parametric oscillator at 710, 725, 740, 750, and 768 nm (PW, 130 fs pulse duration, 82 MHz repetition rate). For reference, a 130 fs pulse

duration corresponds to a 16 nm bandwidth at 800 nm. The effect of CW and PW excitation was compared at 808 nm, with no significant difference in the resulting PL spectra. For this reason do not distinguish between spectra obtained with CW and PW excitation in what follows.

In order to average over a large ensemble of SWNTs, the MPL setup was used with a 100 μm laser spot diameter, sampling $\sim 10^4$ pillars. The many narrow peaks seen with a smaller spot size average out to perhaps ten broad peaks. Spectra resulting from excitation at many different wavelengths are shown in Fig. 3, in each case using an average power of 1.7 mW. Each spectrum is shifted vertically by an amount proportional to the excitation wavelength.

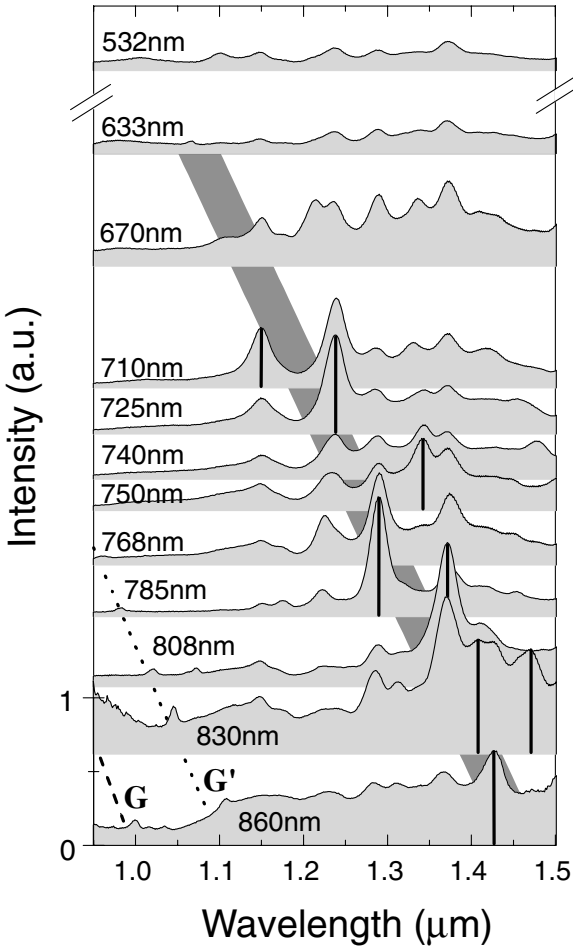

FIG. 3. Excitation wavelength dependence of photoluminescence spectra. Photoluminescence spectra are shown for a series of excitation wavelengths. Spectra were taken at room temperature in air with the MPL configuration using various lasers (see text). A 100 μm spot diameter and an average power of 1.7 mW was used in all cases. Each spectrum is offset along the y axis by an amount proportional to the excitation wavelength. The same laser power and collection optics were used for all spectra so the intensity can be compared for different curves. The thick grey band highlights the expected PL resonance. The black vertical lines highlight PL peaks which are resonant. The dotted and dashed lines trace the G' and G Raman modes, respectively.

Tracing a given peak vertically from spectrum to spectrum, for example, at 1.3 μm, reveals that as the excitation wavelength is increased each peak increases in intensity, reaching a maximum, before decreasing again. Resonant peaks are marked in Fig. 3 with a black line at their center. On average for the marked peaks the ratio of resonant peak wavelength to excitation wavelength is 1.70, with a standard deviation of 0.06. This value for the ratio is also highlighted on the graph with a dark grey band. The resonance occurs in a band about this average because of the chirality dependence of the ratio of first and second singularity wavelengths. While the same PL peaks are seen off resonance, for example, at 532 nm, they are substantially reduced in intensity. The resonance phenomenon confirms that the luminescence is indeed from SWNTs.

Consistent with this picture, at longer excitation wavelengths the G' and G Raman modes of SWNTs and graphite come into view. The theoretically predicted G' band and G band wavelengths [7] are labeled with dotted and dashed lines, respectively. The corresponding Raman peaks are clearly seen.

These results show that bright, narrow PL from SWNTs can be obtained without any postgrowth processing. The PL mechanism is electron-hole recombination through the lowest Van Hove singularities at the band edge. Evidently, previous investigations failed to detect PL from unprocessed nanotubes because interactions between SWNTs and their surroundings can quench luminescence. The comparison between the PL from SWNTs suspended on pillars and the PL from areas in which SWNTs lie on the substrate makes this clear. This is consistent with previous studies in which only individual tubes in aqueous micellar suspensions were observed to luminesce [8,9].

Having optically active SWNTs fixed on a substrate is very useful from the point of view of both materials science and fundamental physics. Photoluminescence characterization, since it is rapid and large scale, should help in the effort to control nanotube diameter and chirality. Already, for these first samples, the presence of a multitude of PL peaks proves that the particular methane CVD process used here, as might be expected, produces a multitude of SWNT species. At least as significantly, as in other materials systems, PL and related techniques can be used in fundamental studies of the physics of SWNTs, monitoring and manipulating their electronic states. Finally, since strong, narrow PL lines can be obtained anywhere in the range 1.0 to 1.6 μm, and most likely beyond, SWNTs have a promising future in optoelectronics, among other applications.

This work was carried out with assistance from the NEDO International Joint Research Grant Program. We

are grateful to R. L. Williams (NRC) and J. Fraser (NRC) for helpful advice regarding PL measurements and to D. Takagi (Meiji University) for performing a series of nanotube depositions.

[1] *Carbon Nanotubes: Synthesis, Structures and Applications*, edited by M. S. Dresselhaus, G. Dresselhaus, and Ph. Avouris (Springer, Berlin, 2001).
[2] P. J. F. Harris, *Carbon Nanotubes and Related Structures* (Cambridge University Press, Cambridge, 1999).
[3] N. Hamada, S. Sawada, and A. Oshiyama, Phys. Rev. Lett. **68**, 1579 (1992).
[4] R. Saito, M. Fujita, G. Dresselhaus, and M. S. Dresselhaus, Appl. Phys. Lett. **60**, 2204 (1992).
[5] J. W. G. Wildöer, L. C. Venema, A. G. Rinzler, R. E. Smalley, and C. Dekker, Nature (London) **391**, 59 (1998).
[6] T. W. Odom, J.-L. Huang, P. Kim, and C. M. Lieber, Nature (London) **391**, 62 (1998).
[7] M. S. Dresselhaus, G. Dresselhaus, A. Jorio, A. G. Souza Filho, and R. Saito, Carbon **40**, 2043 (2002).
[8] M. J. O'Connell, S. M. Bachilo, C. B. Huffman, V. C. Moore, M. S. Strano, E. H. Haroz, K. L. Rialon, P. J. Boul, W. H. Noon, C. Kittrell, J. Ma, R. H. Hauge, R. Bruce Weisman, and R. E. Smalley, Science **297**, 593 (2002).
[9] S. M. Bachilo, M. S. Strano, C. Kittrel, R. H. Hauge, R. E. Smalley, and R. Bruce Weisman, Science **298**, 2361 (2002).
[10] G. U. Sumanasekera, C. K. W. Adu, S. Fang, and P. C. Eklund, Phys. Rev. Lett. **85**, 1096 (2000).
[11] S. V. Kalinin, D. A. Bonnell, M. Freitag, and A. T. Johnson, Appl. Phys. Lett. **81**, 5219 (2002).
[12] Y. Homma, Y. Kobayashi, T. Ogino, and T. Yamashita, Appl. Phys. Lett. **81**, 2261 (2002).
[13] J. Kong, A. M. Cassell, and H. Dai, Chem. Phys. Lett. **292**, 567 (1998).
[14] Y. Homma, T. Yamashita, P. Finnie, M. Tomita, and T. Ogino, Jpn. J. Appl. Phys. **41**, L89 (2002).